
Simplifying the construction concept of the elemented Zollinger roof

Alexander STAHR*, Marius ZWIGART^a, Vladimir MANDTLER^a,
Christian HEIDENREICH^b, André KILIAN^b, Katrin VÖGELE^c

^{*a} HTWK Leipzig, FLEX | Professional Research Team
Karl-Liebknecht-Straße 132, 04277 Leipzig
alexander.stahr@htwk-leipzig.de

^b HTW Dresden, Professorship Statics and Structural Analysis

^cTU Braunschweig,
Institute of Building Construction and Timber Structures

Abstract

The enormous consumption of resources is one of the central issues in construction today. In the context of using wood as a building material, this problem overlaps with the limited availability of natural resources and the risk of loss of biodiversity in the context of extensive wood use. The resource-saving Zollinger roof describes a constructive solution approach in which, by exploiting curvature effects in hall roofs, material savings of around 30% are possible compared to glulam constructions subject to bending stress.

In the context of a comprehensive research project, an experimental roof was realized. In this case, the classic construction principle of the Zollinger roof was further developed so that the construction was assembled from prefabricated shell elements in which the flat roof formwork consists of wood-based panels (LVL). During the implementation of the project, a problem became apparent in the structural-static interaction of the diagonally aligned wooden beams (GL) and the rigid roof panel (LVL). Due to the length tolerances in the NC-supported production of the bar lamellas, the joints between them could sometimes not be carried out in a force-fitting manner. The flat planking of the rib construction “leveled out” this problem and still ensured the integrity of the construction. The question therefore arises as to whether the load-bearing and deformation behavior of the construction will change if the impacts of the ribs are deliberately avoided?

To answer the question, a small series of tests was designed. In four different design variants, 3 large-format uniaxially curved shell elements (test specimens) with the same roof geometry were loaded in the test stand. The results show that the load-bearing effect of the lamellas was significantly overestimated in the previous model assumptions and that a significant increase in load-bearing capacity and stiffness is possible through the flat paneling with wood-based materials. The paper explains the experimental concept and implementation of the experiment as well as it presents and compares the experimental results.

Keywords: Zollinger, ReFlexRoof, micro-step-joint, wood construction, shell structure, lightweight construction, structural design, constructive solution, resource efficiency, static proof, arch roof, board-rip-construction, finite-element-analysis

1. Introduction

The concept of the geometrically and structurally flexible ReFlexRoof roof system for covering halls formed the design basis for the TimberPlan+ research project, which in turn formed the basis for the further work described in this paper. The construction is based on the so-called Zollbau system [1] and has been further developed over the last 10 years in the context of various funded research projects at the HTWK Leipzig with various project partners, including the HTW Dresden and the TU Braunschweig.

A timber frame shell describes a simply curved construction made of diamond-shaped boards with a curved upper side, small cross-section and "hand-assembled" length, which is stiffened over its entire surface by means of the roof formwork or, according to the current state of research, has a load-bearing effect [2][4]. The timber frame shell is always made from the same shaped planks as sawn timber, which are usually approx. 1.90 - 2.5 m long and 14 - 30 cm high. The structural connection of the original Zollinger roof is in the form of a simple bolt with two washers and nuts, which connects one "continuous" and two "offset" slats in a simple manner.

Within the MVK project, this detail of the custom construction method was specifically researched and adapted to the current state of manufacturing technology using joinery machines, as well as structurally and statically improved. As a result, the previous pin is no longer required in favor of a step joint [4].

The special, angled cut of the board ends (shifter cut) codes or generates the continuous curvature in the longitudinal direction of the lamellas that results during assembly. The result is a net-like surface structure of rhombuses arranged next to each other, creating a very decorative roof soffit.

A large-scale demonstrator was constructed as part of the TimberPlan+ research project, see Figure 1. However, further problems came to light here, which primarily concerned the form fit under the lamellae and the form fit during the assembly of the segments used, consisting of several lamellae and parts of the cover shell [10]. The static interaction between the louvres and the cover shell also needs to be clarified further.



Figure 1: Demonstrator based on the ReFlexRoof principle (TimberPlan+)
[FLEX @ HTWK Leipzig, M. Zwigart]

2. Problem description

The prototype, an vaulted roof, which was developed in the research project, was produced using several segmented elements. The elements consist of a large number of so-called Micro Offset Nodes (MVK). These nodes form a load-bearing lamella structure that is spanned by a standardized panel element. The panel is stapled to the lamellas in the factory. To produce the elements, the panel is placed in a prefabricated formwork. This forces the planking into an arch shape. The lamellas are then positioned on the panel and stapled from below. Several of these prefabricated elements were then transported to the construction site and assembled together with the surrounding elements to an arched shape roof. During the construction of the roof, it quickly emerged that the joints could not be connected properly. This resulted in gaps in the nodal points, see Figure 2.

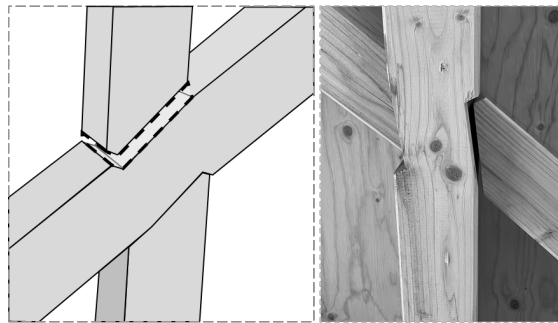


Figure 2: Representation of the gap (left: visualisation of the gap, right: photo from the construction site) [K. Vögele, TU BS]

It is assumed that these gaps were caused due to the recoil forces of the pre-curved planking. This led to a pre-deformation. Furthermore, it cannot be ruled out that the gap resulted from material and manufacturing inaccuracies, which are significantly higher for such spatial complex geometry and structures. These gaps also result in a stiffness alteration in the load-bearing structure, which was analysed within the MVK research project. This has an impact on the entire roof and is therefore relevant to the structural design [11].

3. Analysis of the structural relationship

The roof prototype was analysed on two separate measuring dates. This involved documenting the gaps as well as the moisture content of the timber structure at different points of the prototype. The first measurement was carried out in January 2023. The insights gained from these measurements were presented in a student thesis at iBHolz, TU Braunschweig [10]. The second measurement was then performed in July 2023.

The wood moisture was measured at a depth of 2 cm in the timber structure. The recordings were taken inside the structure as well as at the edge of the structure. However, differences in wood moisture based on the measurement location could not be determined. Temporal differences between winter and summer could be analysed on average depending on the locations in the following table:

Table 1: Differences in temperature and wood moisture

	January 2023	July 2023
Temperature	1.0°C	19.8°C
Average wood moisture	16.3 %	13.5 %

It can be shown that the climate transition had a significant impact on the wood. From January to June, the wood moisture content decreases by 2.8 %. Generally viewed, it is within the range of service class 2 of EC5 [12].

The gaps occurred in different ways. In the following, a representation without the second lamella on the MVK has been chosen to illustrate this fact:

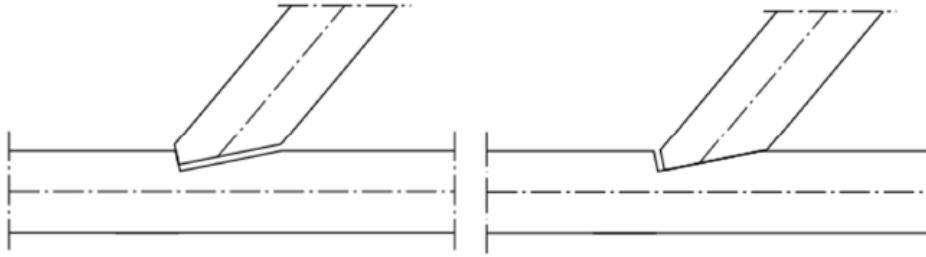


Figure 3: Variation of the gap (left: visualisation of the gap on the bottom notch, right: visualisation of the gap on the front notch) [L. Ghouse, [10]]

The gap appeared on the front notch of the node and in various sceneries also on the bottom notch. In addition, there was also an opening on both notches as shown in Figure 2. Measured was always the gap distance from the bottom notch to the surface of the abounding lamella (Figure 3, left). The reason for this is that the failure of the nodal point occurs if the lamella slips over the front notch.

The relative frequencies of the gap sizes are shown below in Figure 3. In total, there was a gap at 101 out of 490 nodal points. This remained the same over the seasons.

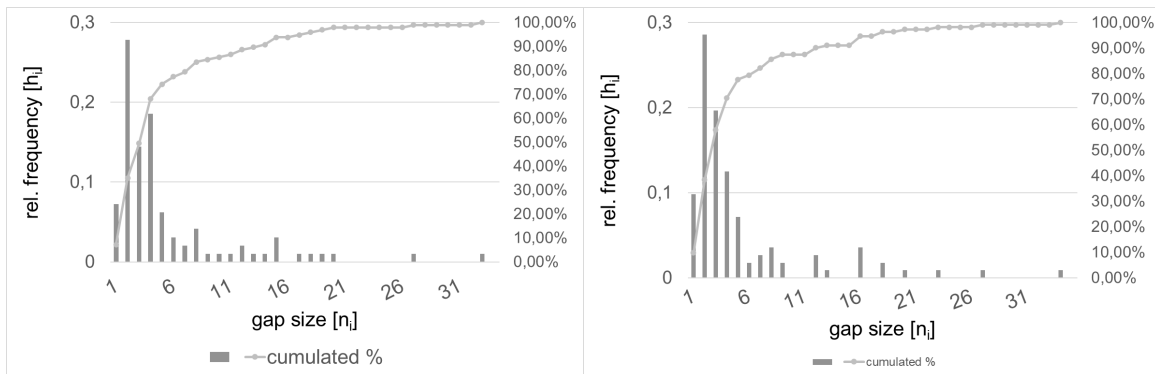


Figure 4: Frequency distributaion of the gaps (left: January 2023 [10], right: July 2023)

Considering the previous diagrams, it can be seen that there was a redistribution of the gap size in July 2023, especially in the gap size range between 10 and 26. On closer analysis, it was discovered that the size of the gaps had decreased in summer. An exact cause for this cannot be given. It is assumed that the drying of the panel could possibly have an effect on the gap size. However, this would require a closer look at the veneer layer of the panel in order to evaluate the effects of shrinkage more precisely. Moreover, the load duration of permanent and quasi-permanent loads cand also have an influence on the gap size. Thus, the entire construction can begin to settle. For this purpose, the measurement have to be extended to include the stitch of the arched shape roof.

4. Hypothesis

In sections 2 and 3 it is shown that the shell construction developed and realized according to the MVK principle (see Figure 1) has considerable gaps in the area of the lamella joints. Despite these gaps, the prototypical large demonstrator structure is fully load-bearing; no major deformations or signs of overloading were detected. It should be noted that the structure was designed for the necessary loads to be applied and was not overdesigned.

On the basis of these preliminary investigations, the main hypothesis can be formulated as follows: The development and dimensioning of the supporting structure as a composite construction consisting of load-bearing lamellae and load-bearing and stiffening cladding exhibits further safety factors that have not yet been sufficiently investigated and taken into account. In addition, the construction can be realized without frictional contact between the lamellae, whereby no conditions restricting the load-bearing function are to be expected. Against this background, a further development of the Zollinger system is

possible with regard to a construction that can be realized with the possibilities of manufacturing accuracy in timber construction, which meets the requirements of a sustainable and flexible construction.

5. Concept of Investigation

5.1. Experimental concept

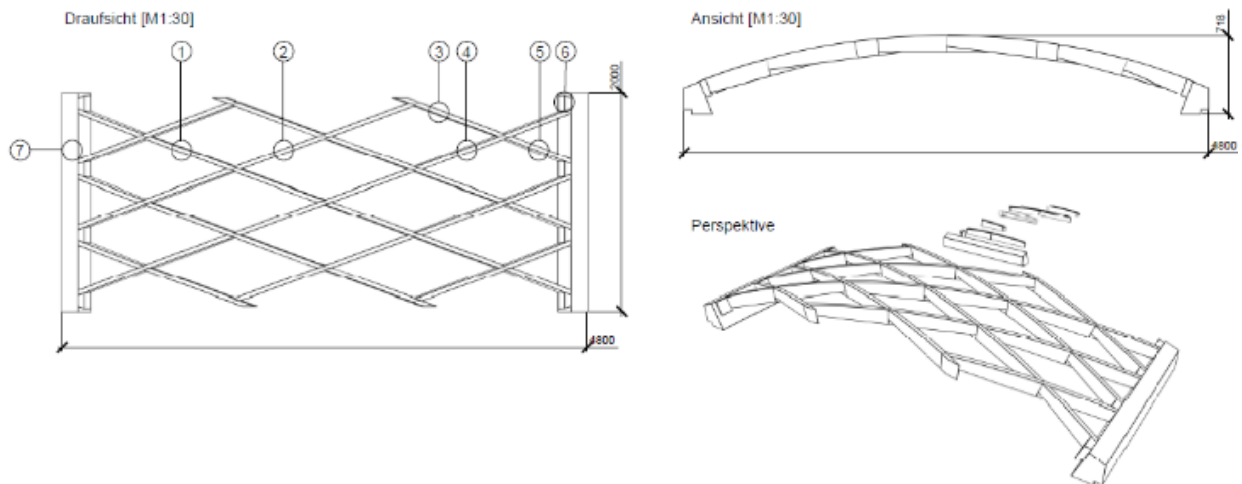


Figure 5: Description of the basic geometry [FLEX @ HTWK Leipzig, L. Franke]

Illustration of test concept: series of tests on large-format test specimens to assess the influence of lamella alignment and lamella contact.

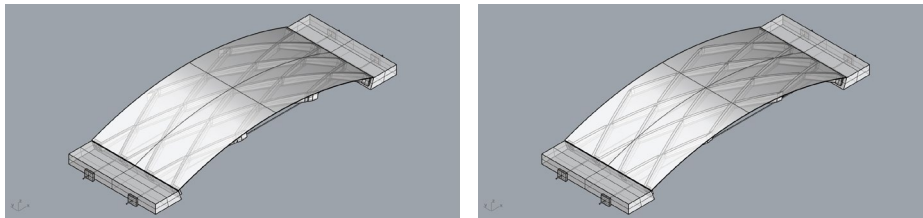


Figure 6: Variants of the roof system (left: V1, right: V2) [FLEX @ HTWK Leipzig, V. Mandtler,]

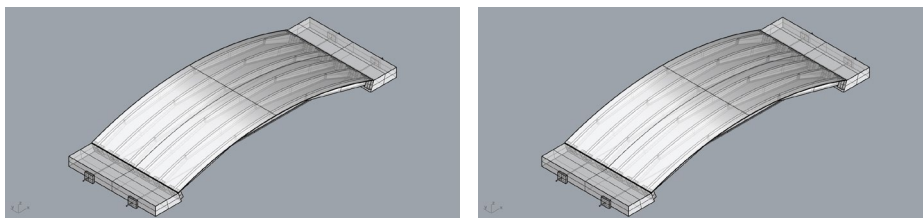
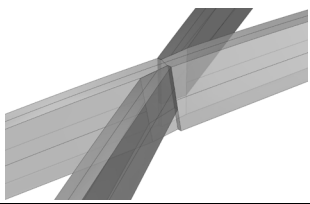
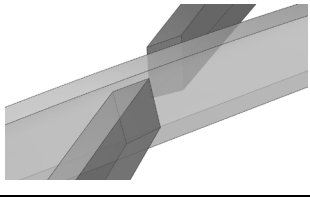
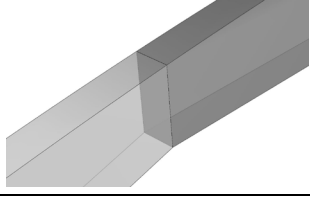
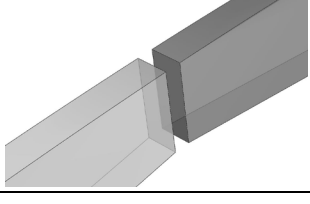


Figure 7: Variants of the roof system (left: V3, right: V4) [FLEX @ HTWK Leipzig, V. Mandtler,]

Table 2: Description of the model variants

Model Nr.	Model description	Detail of connection point (figure)
Type 01	Crossed and connected load bearing lamellas, covered with wood fiber board	
Type 02	Crossed, not connected lamellas, covered with wood fiber board	
Type 03	Parallel and connected load bearing lamellas, covered with wood fiber board	
Type 04	Parallel, not connected lamellas, covered with wood fiber board	

The several times cited previous project "ReFlexRoof" from 2018 was used as a template in terms of geometry and dimensions. Variant one of the "KLIMA-Dach" test series is identical to the test bodies of "ReFlexRoof". The external dimensions of the test specimens, the radii of curvature and the cross-sections of the lamellas, support beams and tension bands are unchanged and the same for all four variants.

Changing the positions of the lamellas and/or the distances between them results in shorter lamella lengths for the remaining three variants.

Material description

- Lamella: K VH, C24, 160 x 40 mm
- Planking: Fundermax® FunderPlan, t = 8 mm
- Support beam: Glulam GL 24h, 200 mm x 600 mm
- Tension strip: S235JR, r = 16 mm
- Staple connections: Prebena Z44CNKHA 44mm, a = 65 mm

Experimental load

In the test, the load is applied as a line load across the entire width of the test body to the row of nodes closest to the one-third point of the arch. A compression fin is used to convert the point load generated by the hydraulic cylinder into a line load. To ensure that the load is applied horizontally throughout, a spherical cap is positioned between the cylinder and the compression fin. The limit load is set at 20 kN.

The measurement data is generated using load cells and displacement transducers. The load cell is placed at the load application point. The displacement transducers sit on the struts of a measuring stand under the test specimens. They measure the vertical displacement of all nodal points of the lamellas and the horizontal displacement of a support beam. The latter measurement is only for control purposes, as the supports are assumed to be immovable in theory due to the tension bands.

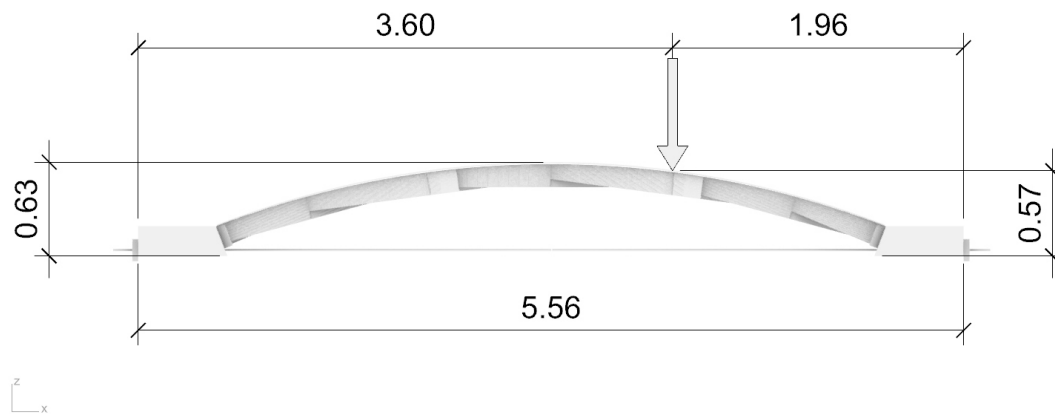


Figure 8: Description of the basic geometry [FLEX @ HTWK Leipzig, V. Mandtler]

5.2. Numerical concept

The experimental model and test concept, see section 5.1, is checked for feasibility and realizability by numerical investigations before the real large load tests are carried out. The four model variants are converted into finite element models and investigated numerically with regard to the basic load-bearing behavior. Furthermore, the quantitative course of the internal forces and the deformation behavior is determined and evaluated comparatively between the model variants. In this way, the physical load tests are optimally prepared with regard to loading and measuring equipment.

5.2.1. FE-implementation of the numerical concept

The numerical calculation models are developed depending on the specifics of the four geometry variants, see Figure 9.

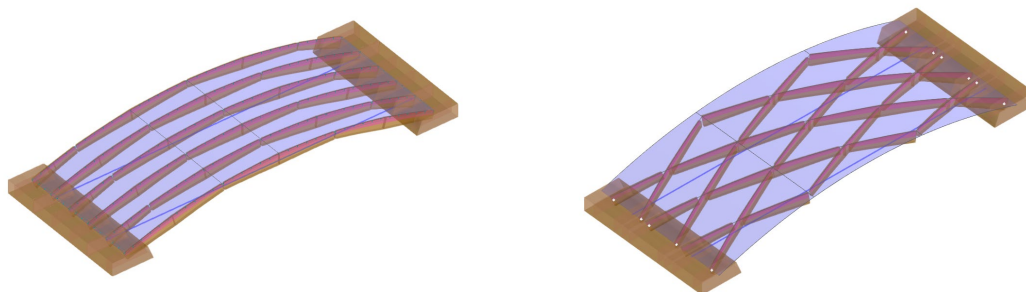


Figure 9: Finite element models (left: parallel lamellae, right: crossed lamellae) [A. Kilian, HTWD]

The calculation of the models is based on the following materials or material types, see table 3.

Table 3: Materials of the elements

Element	Element type	Material	E-Modulus [N/mm ²]	Material type
Lamella	beam	Wood C24	11 000	isotropic – linear
Planking	shell (8 mm)	FunderPlan	4 1000	isotropic – linear

All four variants are modeled as member-surface models using the finite element calculation software RFEM. The individual components are mechanically modeled as follows. The lamellas are considered as bending beams and the planking as a folded structure, for the transmission of membrane loads. The connection between the lamella and the planking are taken into account via staple connections in the form of a line release. The influence of this connection on the overall load-bearing behavior is derived and considered in detail in [9]. Depending on the material parameters to be used for the model tests, the following k_d values can be determined as a function of clamp parameters and distances:

$$K_{ser} = \rho_{mean}^{1.5} \cdot \frac{d_{staple}^{0.8}}{80} \quad (1)$$

$$K_u = \frac{2}{3} \cdot K_{ser} \quad (2)$$

$$K_d = \frac{K_u}{\gamma_M} \quad (\text{with } \gamma_M = 1.3) \quad (3)$$

Table 4: Displacement modulus depending on wood quality, staple leg diameter d and spacing a, see also [9]

d_{staple} [mm]	ρ_{mean} [kg/m ³]	K_{ser} [kN/m]	a [mm]	staple per m	K_{ser} [kN/m ²]	K_u [kN/m ²]	K_d [kN/m ²]
1.5	648	286.25	65	15.38	4388.40	2925.6	2250.46

In variants no. 2 and no. 4, there is no contact between the individual lamellas. They are built with a "gap" in this area. From a static-mechanical point of view, the forces occurring in the lamellas are transmitted via the respective planking areas above them. In these areas, there is a higher load in the area of the planking.

In contrast to the aforementioned variants, variants no. 1 and no. 3 have contact between the lamellas. For the implementation of the finite element models, this connection is simulated as a lamella-lamella contact using bar end joints. The formulation of the degrees of freedom taken into account here is discussed in detail in [9].

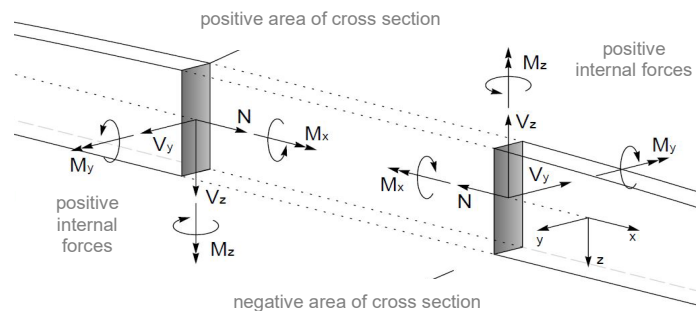


Figure 10: Definition of internal forces [9]

The bar end joints are defined as follows. To take account of the translation, u_x and u_z are defined as rigid in the longitudinal direction and upwards. Tension failure is defined in the x-direction. A spring (5 kN/m) is provided in the transverse direction to ensure numerical stability. A spring (10 kNm/rad) is provided around the transverse axis to account for rotation and ensure numerical stability.

The load is applied as a half-sided load in the form of a line load in the area of the lamella nodal points (approximately in the third points) of the structure in accordance with the test concept, see Figure 11. The level of the load is increased in stages (50 steps), whereby a maximum load of 20 kN is specified in accordance with the test design.

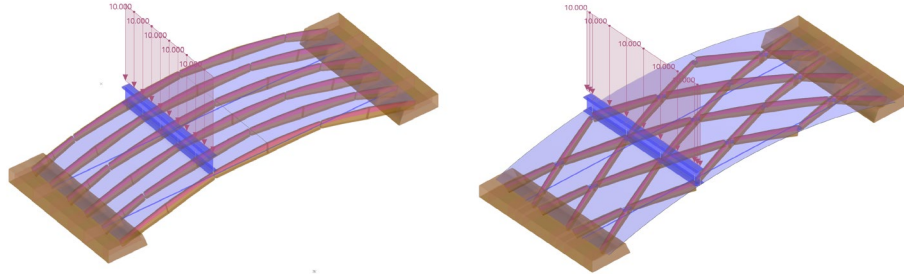


Figure 11: Load positioning [A. Kilian, HTWD]

Due to the large deformations expected and confirmed in preliminary tests, the calculation is carried out according to third-order theory. Equilibrium on the deformed system with consideration of the torsion. The stiffness matrix is determined iteratively.

5.2.2. Results

The finite element analysis of the four model variants analyzed is illustrated below using selected results. The vertical deformation u_z of a selected node and the normal force in a lamella element, see Figure 12, are compared. Due to the incremental load increase, the behavior of the structure can be simulated in the course of the load test.

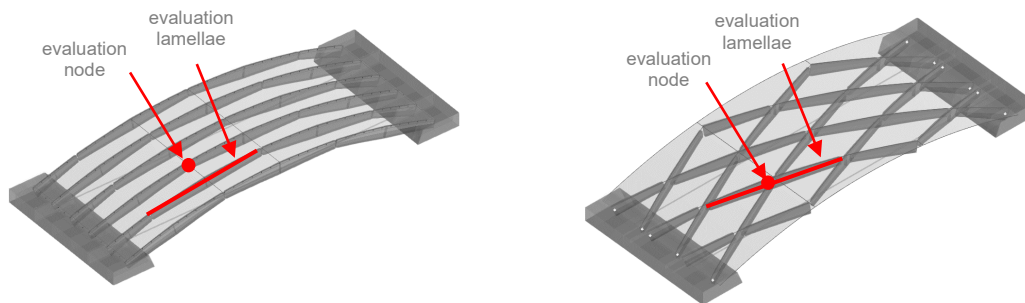


Figure 12: Evaluation node and lamellae of the variants (left: parallel lamellae, right: crossed lamellae) [HTW Dresden, A. Kilian]

Figure 13 shows the load-deformation behavior of the four variants. The maximum load was set at 20 kN, which is applied in increments. It is clear that the variants with connected slats (no. 1 and no. 3) have smaller deformations than the variants with unconnected slats (no. 2 and no. 4).

The load-deformation behavior of variants no. 1 and no. 3 is attributed to the higher stiffness due to the interaction between the slats and the load-bearing cladding. In variants without a connection between the slats (variant no. 2 and no. 4), the forces cannot be transmitted over the entire length of the slats and are transferred via the cladding. The slats therefore act primarily as buckling reinforcement.

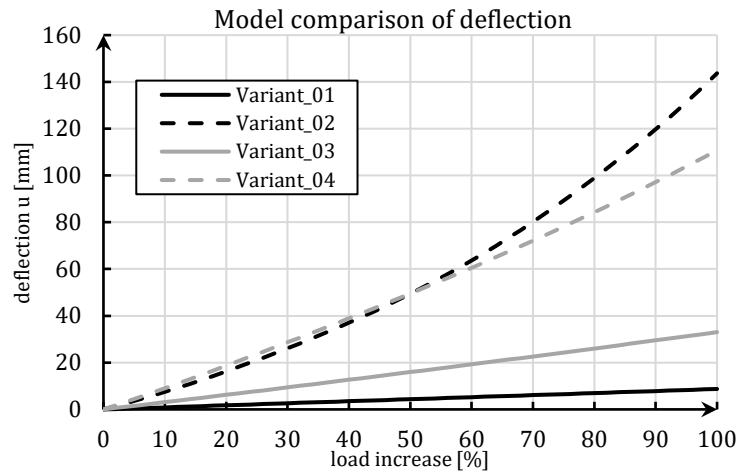


Figure 13: Vertical deformation of the 4 variants due to load increase [HTW Dresden, A. Kilian]

Figure 14 shows the internal forces in the form of normal forces of selected lamella areas as a function of the load increase. This clearly shows that the normal tensile forces of the models without lamella connections in the middle of the lamella are greater than those variants without lamella connections. This is due to the fact that a compression arch is formed and thus a more even distribution of force is achieved, which reduces the normal tensile force. The effect of the compression bow can be clearly seen in the deformation images of the jointless models, as the deformation is smaller.

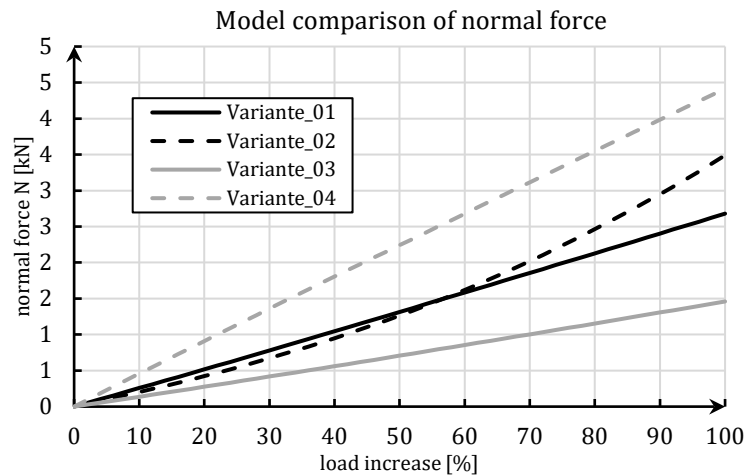


Figure 14: Vertical deformation of the 4 variants due to load increase [HTW Dresden, A. Kilian]

Furthermore, Figure 14 clearly shows that non-linear load-deformation diagrams are created, especially for the variants with joints. From approx. 60 % of the total load, the deformation and the internal forces increase significantly.

In addition to the analyses of the deformations and internal forces in selected areas, the specific timber construction details must also be verified. The following verifications should be mentioned as examples: Normal stress verification, buckling verification, normal force and bending verification and connection verification.

In the course of further numerical investigations, an imperfection must be applied, especially for the parallel lamellas, which takes into account possible production and material-related perpendicular deviations. In conclusion, it should be noted that the variants with a contact between the lamellas exhibit lower deformations. Against this background, the variant envisaged here should be investigated further with regard to the simpler manufacturing and joining properties.

6. Summary and Outlook

This article presents a further optimization of timber lattice shell structures according to the Zollinger principle. The main focus here is on the timber construction-specific connection points of the lamellae against the background of the manufacturing and joining technology.

The design variants investigated are characterized by the connection points between the lamella-lamella and lamella-planking. It can be shown that the deformations due to the load in the vertical direction can be reduced using the modeled mathematical approach of contact between the lamellas. Taking into account an economical design and the specifics of typical timber structures, the variants without contact between the lamellas represent a sensible alternative that requires further investigation.

The numerically determined results should be checked and verified in further physical load tests. If necessary, the model approaches have to be re-calibrated. The results obtained as a result of the load tests under the given boundary conditions (span, height, component measurements, materials, half-sided load) must be checked for transferability to other system parameters. In this way, the universal approach of the concept shown here can be tested.

Acknowledgements

The German Federal Ministry of Food and Agriculture (Agency for sustainable raw materials) funded the project (funding code: 2220HV003). The authors are responsible for the content of this publication.

References

- [1] F. Zollinger: “Raumabschließende, ebene oder gekrümmte Bauteile”. Patent 387469, 1921.
- [2] L. Franke, A. Stahr, A. Dijoux and A. Heidenreich, „How Does the Zollinger Node Really Work?“, in: *Proceedings of the IASS Symposium 2017*, Hamburg, 2017.
- [3] C. Dijoux, A. Stahr, L. Franke and C. Heidenreich, “Parametric Engineering of a Historic Timber-Gridshell-System”, in *Proceedings of the IASS Symposium 2017*, Hamburg, 2017.
- [4] A. Stahr, C. Dijoux, L. Franke, M. Tremel and J. Bialozyt, „Der Mikroversatzknoten - eine innovative Holzverbindung“, *Bauen mit Holz*, Vol. 3.2019, S. 22–29.
- [5] A. Stahr, C. Dijoux, L. Franke and M. Tremel, “Brettriependächer in elementierter Bauweise”, *Bauen mit Holz*, Vol. 7/8, 2019, S. 20-27.
- [6] A. Stahr, C. Dijoux and M. Dembski, “Zollinger – Ein Flachdach der etwas anderen Art”, *Flachdächer*, Ernst & Sohn Special 2019, S. 23-28
- [7] A. Stahr, C. Heidenreich, A. Kilian, C. Dijoux, L. Franke and R. Hallahan, “Load test on ribbed timber shells for medium span roofs”, in *Proceedings of the IASS Symposium 2020/21*, Guilford, 2021.
- [8] C. Heidenreich, A. Kilian, J. Büttner and S. Scherer, “Derivation of wind loads for shell structures using CFD analyses”, in *Proceedings of the IASS Symposium 2023*, Melbourne, 2023
- [9] C. Heidenreich, J. Büttner and A. Kilian, “Static Modelling and Analyses of Ribbed Timber Shell Roof Structures”, in *Journal of the IASS*, Vol. 65 (2024) No. 2 June n. 220
- [10] L. Ghouse, “Statistische Beurteilung von fertigungstechnischen Maßtoleranzen in einem neuartigen Dachtragwerk mit Bewertung von Maßnahmen zur Optimierung in der Fertigung und Montage“, Bachelorarbeit, TU Braunschweig, 2023.
- [11] K. Vögele, M. Tronnier, Y. Plüss, M. Sieder, “Structural characteristics and deformation behaviour of an advanced carpentry connection in timber construction”, in *Proceedings of the World Conference on Timber Engineering 2023*, Oslo, 2023.
- [12] *Eurocode 5: Design of timber structures – Part 1-1: General – Common rules and rules for buildings*, DIN EN 1995-1-1:2004, CEN, December 2010.